



## NEUROBIOLOGY

# The Bradykinin B<sub>1</sub> Receptor Regulates A $\beta$ Deposition and Neuroinflammation in Tg-SwDI Mice

Giselle F. Passos,\* Rodrigo Medeiros,\*<sup>†</sup> David Cheng,\*<sup>†</sup> Vitaly Vasilevko,\* Frank M. LaFerla,\*<sup>†</sup> and David H. Cribbs\*<sup>‡</sup>

From the Institute for Memory Impairments and Neurological Disorders\* and the Departments of Neurobiology and Behavior<sup>†</sup> and Neurology,<sup>‡</sup> University of California, Irvine, Irvine, California

Accepted for publication  
January 8, 2013.

Address correspondence to  
Giselle F. Passos, Ph.D., Institute  
for Memory Impairments and  
Neurological Disorders, Univer-  
sity of California, Irvine, 1226  
Gillespie Neuroscience Research  
Facility, Irvine, CA 92697-4540;  
or David H. Cribbs, Ph.D.,  
Institute for Memory Impair-  
ments and Neurological Disor-  
ders and the Department of  
Neurology, Neuropathology  
Core, Alzheimer's Disease  
Research Center, University of  
California, Irvine, 1111 Gillespie  
Neuroscience Research Facility,  
Irvine, CA 92697-4540.  
E-mail: gf.passos@uci.edu or  
cribbs@uci.edu.

The deposition of amyloid- $\beta$  peptides (A $\beta$ ) in the cerebral vasculature, a condition known as cerebral amyloid angiopathy, is increasingly recognized as an important component leading to intracerebral hemorrhage, neuroinflammation, and cognitive impairment in Alzheimer disease (AD) and related disorders. Recent studies demonstrated a role for the bradykinin B<sub>1</sub> receptor (B<sub>1</sub>R) in cognitive deficits induced by A $\beta$  in mice; however, its involvement in AD and cerebral amyloid angiopathy is poorly understood. Herein, we investigated the effect of B<sub>1</sub>R inhibition on AD-like neuroinflammation and amyloidosis using the transgenic mouse model (Tg-SwDI). B<sub>1</sub>R expression was found to be up-regulated in brains of Tg-SwDI mice, specifically in the vasculature, neurons, and astrocytes. Notably, administration of the B<sub>1</sub>R antagonist, R715, to 8-month-old Tg-SwDI mice for 8 weeks resulted in higher A $\beta$ <sub>40</sub> levels and increased thioflavin S—positive fibrillar A $\beta$  deposition. Moreover, blockage of B<sub>1</sub>R inhibited neuroinflammation, as evidenced by the decreased accumulation of activated microglia and reactive astrocytes, diminished NF- $\kappa$ B activation, and reduced cytokine and chemokine levels. Together, our results indicate that B<sub>1</sub>R activation plays an important role in limiting the accumulation of A $\beta$  in AD-like brain, likely through the regulation of activated glial cell accumulation and release of pro-inflammatory mediators. Therefore, the modulation of the receptor may represent a novel therapeutic approach for AD. (*Am J Pathol* 2013, 182: 1740–1749; <http://dx.doi.org/10.1016/j.ajpath.2013.01.021>)

The progressive accumulation of amyloid- $\beta$  (A $\beta$ ) in the brain is a prominent feature of Alzheimer disease (AD) and related disorders, together with neurofibrillary tangles, cognitive decline, and chronic inflammation.<sup>1,2</sup> A $\beta$  is a 36– to 43–amino acid peptide, which is produced by sequential enzymatic cleavage of the amyloid precursor protein (APP) by  $\beta$ - and  $\gamma$ -secretases.<sup>1</sup> Overproduction, altered processing, or failure of clearance by cellular uptake and degradation or transport across the blood-brain barrier (BBB) have been shown to cause the accumulation of A $\beta$  in the form of plaques in brain parenchyma and in walls of cerebral vessels as cerebral amyloid angiopathy (CAA).<sup>3,4</sup> In contrast to parenchymal plaques, which can be composed of either diffuse or fibrillar deposits, cerebral vascular A $\beta$  deposits are largely of fibrillar form.<sup>5</sup> Several studies have shown that cerebral vascular A $\beta$  deposits are associated with a localized neuroinflammatory response and cognitive impairment, and

it has been suggested that microvascular A $\beta$  accumulation is a better correlate with dementia than parenchymal amyloid plaques in individuals with AD and CAA.<sup>6–11</sup>

CAA is the major pathological feature of several familial disorders involving specific point mutations within the A $\beta$  region of the APP gene, including the Dutch type (E22Q) and the Iowa type (D23N), which cause early and severe cerebral vascular amyloid deposition.<sup>12–14</sup> A transgenic mouse model (Tg-SwDI) has been generated expressing human Swedish/Iowa triple-mutant APP in the brain.<sup>15</sup> The resulting

Supported by National Institute of Aging grant AG020241 (D.H.C.), National Institute of Neurological Disorders and Stroke grant NS050895 (D.H.C.), Program Project grant PO1 AG00538 (F.M.L. and D.H.C.), and Alzheimer's Association grant IIRG11-204835 (D.H.C.). Anti-A $\beta$ <sub>40</sub> and anti-A $\beta$ <sub>42</sub> antibodies and A $\beta$ <sub>40</sub> and A $\beta$ <sub>42</sub> peptides were provided by the University of California, Irvine, Alzheimer's Disease Research Center through funding from NIH/National Institute of Aging grant P50 AG16573.

Dutch/Iowa mutant A $\beta$  presents highly vasculotropic properties and low efficiency for BBB transport, thus resulting in early-onset and robust deposition of cerebral microvascular amyloid and diffuse parenchymal A $\beta$ .<sup>16–18</sup> In addition, Tg-SwDI mice exhibit marked neuroinflammation and behavioral deficits, providing a valuable experimental paradigm to study selective accumulation of cerebral vascular amyloid and potential therapeutic interventions in CAA.<sup>19,20</sup>

Kinins are a family of biologically active peptides generated at the sites of tissue damage in response to trauma or infection, or during most inflammatory processes.<sup>21</sup> The role of kinins has been described in numerous systems, and their main pharmacological effects include smooth muscle contraction and relaxation, vasodilatation, increase in vascular permeability, cell recruitment, and sensitization of nociceptive fibers.<sup>22–24</sup> Kinins exert their actions through the stimulation of two different G-protein-coupled receptors, classified as B<sub>1</sub> and B<sub>2</sub>.<sup>24</sup> The B<sub>2</sub> receptor is constitutively expressed in central and peripheral mammalian tissues, mediating most of the physiological actions evoked by kinins and exhibiting high affinity for bradykinin and kallidin. In contrast, the B<sub>1</sub> receptor (B<sub>1</sub>R) shows higher affinity for the metabolites des-Arg<sup>9</sup>-bradykinin and des-Arg<sup>10</sup>-kallidin and is present at low levels under normal conditions, but can be strongly up-regulated after tissue trauma, during certain inflammatory states, or by the action of pro-inflammatory cytokines or bacterial products.<sup>25</sup> Therefore, inappropriate B<sub>1</sub>R expression has been suggested to have a pivotal role in several chronic diseases involving pain and inflammation.<sup>22,23,26</sup> Recently, it has been demonstrated that the intracerebral administration of A $\beta$ <sub>40</sub> in rodents results in up-regulation of B<sub>1</sub>R expression in brain regions related to cognitive behavior, and that blockade of B<sub>1</sub>R signaling improves A $\beta$ -induced cognitive deficits, suggesting the involvement of the kinin system in AD.<sup>27–29</sup>

Given the important role of B<sub>1</sub>R in mediating vascular function and inflammatory processes, in the present study, we investigated the effect of selective pharmacological blockade of B<sub>1</sub>R on A $\beta$  deposition and neuroinflammation in Tg-SwDI mice. We observed a marked up-regulation of the receptor expression in Tg-SwDI brains, and the blockade of B<sub>1</sub>R activation resulted in increased fibrillar A $\beta$  deposition. In addition, we found a reduced neuroinflammatory response in mice treated with the B<sub>1</sub>R antagonist, as demonstrated by a marked decrease of microglial and astrocytic activation and diminished levels of pro-inflammatory mediators. Together, these results provide evidence that the B<sub>1</sub>R is involved in the regulation of A $\beta$  deposition and neuroinflammation, and suggest that this receptor could be a new target for the treatment of AD.

## Materials and Methods

### Animals and Treatments

Tg-SwDI line B mice that express the human APP770 cDNA containing the Swedish (KM670/671NL), Dutch (E693Q),

and Iowa (D694N) mutations were used in this study.<sup>15,20</sup> Tg-SwDI mice and non-transgenic (nTg) C57Bl/6 mice ( $n = 8$  for each group) were 8 months of age at the beginning of the study. All experiments followed the NIH guidelines and were approved by the University of California, Irvine, Institutional Animal Care and Use Committee.

The pharmacological modulation of the B<sub>1</sub>R was performed using 1 mg/kg selective antagonist Ac-Lys-[D- $\beta$  Nal,<sup>7</sup> Ile<sup>8</sup>] des-Arg<sup>9</sup>-bradykinin (R715; Biomatik, Wilmington, DE), given as daily s.c. injections for 8 weeks.<sup>30,31</sup> Control mice received vehicle (0.9% NaCl solution).

### Behavioral Tests

Novel object and novel place recognition tests were used to evaluate cognition. Each mouse was habituated to an empty arena for 5 minutes 1 day before testing. On the first day of novel object testing, mice were exposed to two identical objects placed at opposite ends of the arena for 5 minutes. Twenty-four hours later, the mouse was returned to the arena, this time with one familiar object and one novel object. Time spent exploring the objects was recorded for 5 minutes. For the place recognition test, each mouse was placed in the arena with two identical objects evenly spaced, and allowed to explore for 5 minutes. After 24 hours, mice were placed in the arena for 5 minutes with one object displaced to a new location, whereas the other object was not moved. The recognition index represents the percentage of the time that mice spend exploring the novel or moved object. Objects used in this task were carefully selected to prevent preference or phobic behavior.

### Tissue Preparation

Mice were deeply anesthetized with sodium pentobarbital and euthanized by transcardial perfusion with 0.1 mol/L ice-cold PBS solution (pH 7.4). The right brain hemispheres were fixed for 24 hours in 4% paraformaldehyde and cryoprotected in 30% sucrose for immunohistochemical (IHC) analysis. Frozen brains were divided into sections coronally (40  $\mu$ m thick) using a Leica SM2010R freezing microtome (Leica Microsystems, Bannockburn, IL), serially collected in cold 0.02% sodium azide in PBS, and stored at 4°C. The left hemispheres were snap frozen on dry ice and subjected to protein extraction using the T-PER tissue protein extraction reagent (Thermo Scientific, Rockford, IL) and 70% formic acid. The supernatant was divided and stored at –80°C. The protein concentration in the supernatant was determined using the BCA Protein Assay kit (Thermo Scientific).

### Western Blot Analysis

Equal protein amounts were separated on a 4% to 12% SDS-PAGE gradient, transferred to a nitrocellulose membrane, and incubated overnight with primary antibodies at 4°C. The following primary antibodies were used: human APP-CT20,

disintegrin and metalloproteinase domain—containing protein (ADAM)10, ADAM17,  $\beta$ -site APP-cleaving enzyme 1 (BACE1; Calbiochem, San Diego, CA), glyceraldehyde-3-phosphate dehydrogenase (GAPDH), B<sub>1</sub>R (Santa Cruz Biotechnology, Santa Cruz, CA), low-density lipoprotein receptor—related protein 1 (LRP1), apolipoprotein E (APOE), neprilysin (Abcam, Cambridge, MA), phosphorylated-p65 NF- $\kappa$ B, liver X receptor, peroxisome proliferator-activated receptor  $\gamma$ , and matrix metalloproteinase-9 (Cell Signaling Technology, Danvers, MA). After washing, the membranes were incubated with adjusted secondary antibodies coupled to horseradish peroxidase. The immunocomplexes were visualized using the SuperSignal West Pico Kit (Thermo Scientific). Band density measurements were obtained using ImageJ imaging software version 1.36b (NIH, Bethesda, MD).

### ELISA Analysis

For the determination of A $\beta$  levels, T-PER soluble fractions were loaded directly onto enzyme-linked immunosorbent assay (ELISA) plates, whereas the formic acid supernatants (insoluble fractions) were diluted 1:40 in a neutralization buffer (1 mol/L Tris base and 0.5 mol/L NaH<sub>2</sub>PO<sub>4</sub>) before loading. Immulon 2HB immunoassay plates (Thermo Scientific) were coated with mAb20.1 antibody at a concentration of 25  $\mu$ g/mL in coating buffer (0.1 mol/L NaHCO<sub>3</sub>/Na<sub>2</sub>CO<sub>3</sub> buffer, pH 9.6) and blocked with 3% bovine serum albumin (BSA). Standard solutions for both A $\beta$ <sub>40</sub> and A $\beta$ <sub>42</sub> were made in antigen capture buffer (20 mmol/L Na<sub>3</sub>PO<sub>4</sub>, 2 mmol/L EDTA, 0.4 mol/L NaCl, 0.05% 3-[(3-cholamidopropyl)dimethylammonio]propanesulfonate, 1% BSA, and 0.05% sodium azide, pH 7.0) and loaded onto ELISA plates in duplicate. Samples were then loaded (in duplicate) and incubated overnight at 4°C. Plates were washed and probed with either biotinylated monoclonal anti-A $\beta$ <sub>40</sub> (C49) or anti-A $\beta$ <sub>42</sub> (D32) antibodies (Alzheimer's Disease Research Center at the University of California, Irvine) in detection buffer (20 mmol/L Na<sub>3</sub>PO<sub>4</sub>, 0.4 mol/L NaCl, 2 mmol/L EDTA, 1% BSA, and 0.002% thimerosal, pH 7.0) overnight at 4°C. Streptavidin—horseradish peroxidase (1:4000; Thermo Scientific) in detection buffer was added and incubated at 37°C for 4 hours. Plates were developed with the addition of Ultra TMB-ELISA substrate (Thermo Scientific), followed by 0.8 mol/L O-phosphoric acid to stop the reaction. The plates were read at 450 nm using a plate reader (Molecular Dynamics, Sunnyvale, CA). The readings obtained were normalized to the protein concentration of the samples.

### Cytokine Protein Array

The expression of multiple cytokines/chemokines was assessed using the Proteome Profiler mouse cytokine array panel A (R&D Systems, Minneapolis, MN), according to manufacturer's instructions. Densitometric analysis of the dot blots was performed using ImageJ version 1.36b (NIH).

### IHC Data

Antigen retrieval was optimized using a 90% formic acid solution for 7 minutes for A $\beta$  staining. Free-floating sections were pretreated with 3% hydrogen peroxide and 10% methanol in Tris-buffered saline (TBS) for 30 minutes to block endogenous peroxidase activity. After a TBS wash, sections were incubated once in 0.1% Triton X-100 (Fisher Scientific, Pittsburgh, PA) in TBS for 15 minutes and once with 2% BSA in 0.1% Triton-X in TBS for 30 minutes. Sections were then incubated overnight at 4°C with biotinylated anti-A $\beta$ <sub>42</sub> (D32) or anti-A $\beta$ <sub>40</sub> (C49) antibodies, or with anti-glial fibrillary acidic protein (GFAP; Millipore, Billerica, MA), anti-CD68, anti-CD11b, or anti-CD45 (IBL-3/16; AbD Serotec, Raleigh, NC) antibodies with 5% normal serum in TBS. After incubation with the appropriate biotinylated secondary antibody for 2 hours, sections were processed using the Vectastain Elite ABC reagent and 3,3'-diaminobenzidine (Vector Laboratories, Burlingame, CA), according to the manufacturer's instructions. Sections were then mounted on gelatin-coated slides, dehydrated in graded ethanol, cleared in xylene, and coverslipped with DPX mounting medium (VWR International, Poole, UK).

The immunostaining was assessed at six brain coronal levels. Specifically, six alternate sections (40  $\mu$ m thick) of the brain, with an individual distance of approximately 160  $\mu$ m, were obtained between 1.34 and 2.54 mm posterior to the bregma. Images of stained subiculum, hippocampus, dentate gyrus, frontotemporal cortex, and thalamus were acquired using an AxioCam digital camera and AxioVision software version 4.6 connected to an Axioskop 50 microscope (Carl Zeiss MicroImaging, Thornwood, NY). The obtained images were analyzed using ImageJ 1.36b (NIH), and data are reported as the labeled area captured (positive pixels)/the full area captured (total pixels). All assessments were performed by examiners (G.F.P. and R.M.) blinded to sample identities.

### Immunofluorescence

Sections were first blocked with 3% normal serum, 2% BSA, and 0.1% Triton X-100 in TBS for 1 hour at room temperature. By using the same buffer solution, sections were incubated overnight at 4°C with the following primary antibodies: anti-A $\beta$ 1-16 (6E10; Covance Research Products, San Diego, CA), anti-collagen IV, anti-GFAP (Abcam), anti-Iba-1 (Wako Chemicals, Richmond, VA), anti-NeuN (Millipore), and/or anti-B<sub>1</sub>R (Novus Biologicals, Littleton, CO). In some experiments, sections were also incubated with biotinylated tomato lectin (Vector Laboratories). Sections were then rinsed and incubated for 1 hour at room temperature with secondary Alexa Fluor—conjugated antibodies (Invitrogen, Carlsbad, CA) or Alexa Fluor—conjugated streptavidin (Molecular Probes, Eugene, OR), when needed. Finally, sections were mounted onto gelatin-coated slides in Fluoromount-G (Southern Biotech, Birmingham, AL) and examined under a Leica DM2500 confocal laser microscope using Leica Application Suite

Advanced Fluorescence software version 2.6.0 (Leica Microsystems, Wetzlar, Germany).

### Thioflavin S Staining

Sections were incubated with 0.5% thioflavin S in 50% ethanol for 10 minutes, washed twice with 50% ethanol, followed by washing with PBS solution. Staining was visualized under a confocal microscope. Image measurements

were made using ImageJ version 1.36b (NIH). The thioflavin S levels represent the average value obtained by the analysis of images of the subiculum, dentate gyrus, and thalamus.

### Statistical Analysis

All data are expressed as means  $\pm$  SEM. Statistical evaluation of the results was performed using one- or two-way analysis of variance. After significant analyses of variance, multiple post hoc comparisons were performed using Bonferroni's test. Some data were analyzed using the unpaired *t*-test. The accepted level of significance for the tests was  $P < 0.05$ . All tests were performed using the Statistica software package (StatSoft Inc., Tulsa, OK).

## Results

### Bradykinin B<sub>1</sub>R Expression Is Up-Regulated in Tg-SwDI Brain

In a first set of experiments, we assessed the expression of B<sub>1</sub>R in brains from 10-month-old nTg C57Bl/6 and Tg-SwDI mice using Western blot and immunofluorescence confocal analyses. The B<sub>1</sub>R was constitutively expressed in nTg mice, primarily in neurons. In contrast, strikingly increased levels of B<sub>1</sub>R were observed in Tg-SwDI brains, with neurons, astrocytes, and vascular cells expressing elevated levels of the receptor (Figure 1, A–C). Notably, up-regulation in B<sub>1</sub>R expression was found in subiculum, dentate gyrus, cortex, and thalamus (Figure 1D). Moreover, B<sub>1</sub>R expression up-regulation was found to be widely associated with A $\beta$  deposition, as demonstrated by confocal colocalization analysis of B<sub>1</sub>R, vasculature (tomato lectin), and A $\beta$  (6E10) (Figure 1E). Taken together, these data demonstrate that A $\beta$  deposition is linked to the up-regulation of B<sub>1</sub>R, suggesting a role for this receptor in the neuropathological alterations observed in the Tg-SwDI model.

### Bradykinin B<sub>1</sub>R Up-Regulation Affects A $\beta$ Deposition

The Tg-SwDI mice are characterized by early-onset and robust accumulation of A $\beta$  in the brain, predominantly in the cerebral

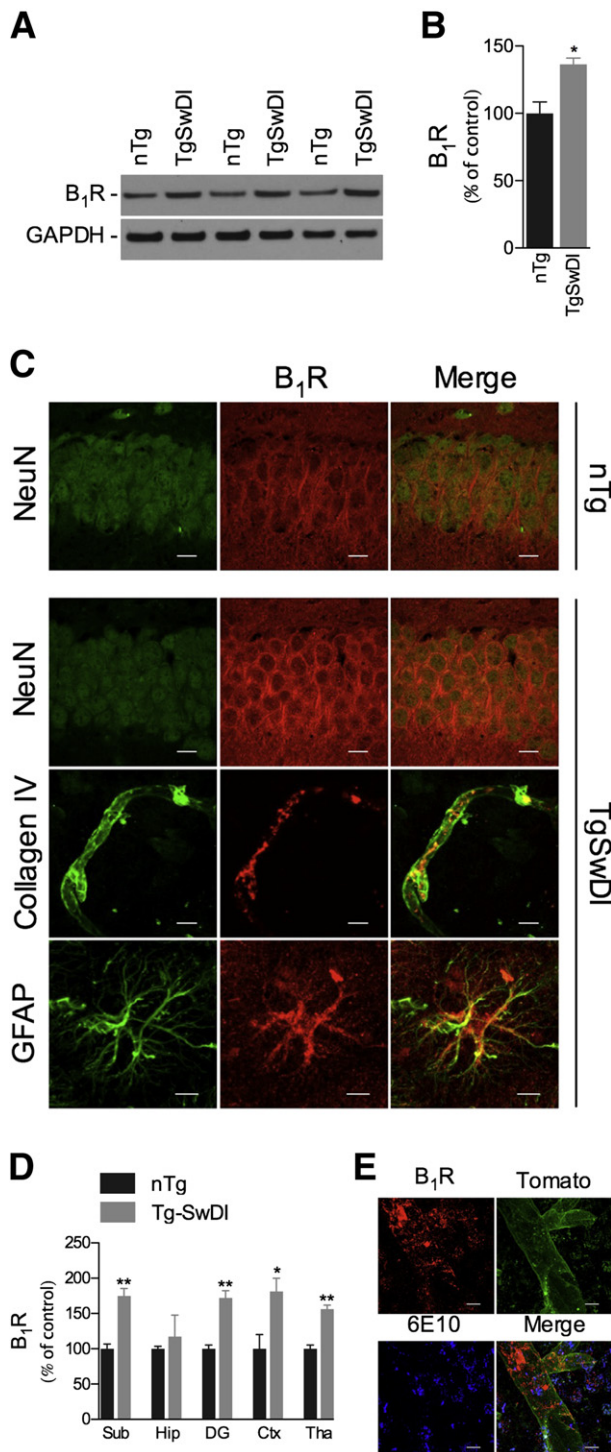


**Figure 1** B<sub>1</sub>R is up-regulated in Tg-SwDI brain. Representative blots (A) and quantitative results (B) of Western blot analysis showing the increased expression of B<sub>1</sub>R in the brains of 10-month-old Tg-SwDI mice compared with age-matched nTg animals. GAPDH levels were used as loading controls. C: In nTg mice, confocal analysis demonstrated the colocalization of B<sub>1</sub>R (red) and NeuN-positive (green) neurons, and elevated immunoreactivities of B<sub>1</sub>R (red) colocalized with NeuN-positive neurons, collagen IV-positive vessels, and GFAP-positive astrocytes (all green) were observed in Tg-SwDI mice. Representative photomicrographs were taken from hippocampus (Hip; NeuN/B<sub>1</sub>R), dentate gyrus (GFAP/B<sub>1</sub>R), and thalamus (collagen IV/B<sub>1</sub>R). D: B<sub>1</sub>R immunoreactivity was increased in cortex (Ctx), thalamus (Tha), dentate gyrus (DG), and subiculum (Sub) of Tg-SwDI versus nTg mice. E: Confocal laser microscopy of B<sub>1</sub>R (red), tomato lectin (green), and 6E10 (blue) demonstrated the colocalization of the B<sub>1</sub>R and the vasculature in areas of A $\beta$  deposits (6E10) in the brains of Tg-SwDI mice. Representative photomicrographs were taken from the thalamus. Scale bar = 10  $\mu$ m. The values represent means  $\pm$  SEM ( $N = 5$  to  $6$ ). \* $P < 0.05$ , \*\* $P < 0.01$ .

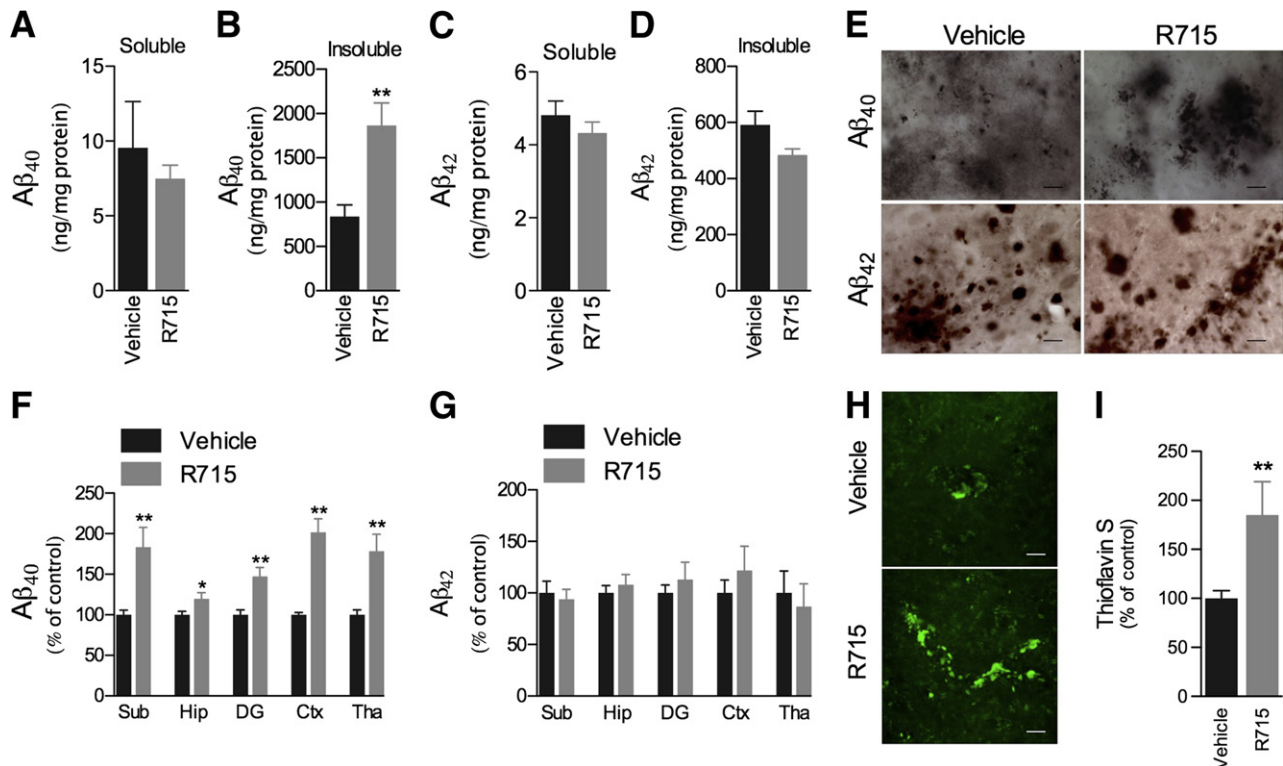


**Figure 2** B<sub>1</sub>R up-regulation affects Aβ deposition in Tg-SwDI brain. Mice s.c. treated with 1 mg/kg R715 for 8 weeks have no changes in the levels of Aβ<sub>40</sub> in the detergent-soluble fraction (A), whereas increased levels of Aβ<sub>40</sub> were observed in the detergent-insoluble fraction (B), and both detergent-soluble (C) and detergent-insoluble (D) Aβ<sub>42</sub> levels remained unchanged, as measured by ELISA. E and F: Aβ<sub>40</sub> immunoreactivity was increased in cortex (Ctx), thalamus (Tha), hippocampus (Hip), dentate gyrus (DG), and subiculum (Sub) of R715-treated mice when compared with the vehicle-treated group. E and G: R715 administration had no effect on Aβ<sub>42</sub> immunoreactivity in Tg-SwDI brains. Representative photomicrographs (H) and quantitative results (I) demonstrating increased thioflavin S-positive fibrillar Aβ deposits in R715-treated mice. Representative photomicrographs were taken from subiculum (E) and thalamus (H). Scale bars: 10 μm (E); 15 μm (H). The values represent means ± SEM (N = 5 to 6). \*P < 0.05, \*\*P < 0.01.

microvasculature.<sup>15,17</sup> To assess the possible role of B<sub>1</sub>R in Aβ deposition in Tg-SwDI mice, we next determined the levels of Aβ<sub>40</sub> and Aβ<sub>42</sub> peptides in both detergent-soluble and detergent-insoluble fractions by ELISA. The s.c. administration of 1 mg/kg selective B<sub>1</sub>R antagonist R715 for 8 weeks, initiated at 8 months of age, resulted in a significant increase in the levels of Aβ<sub>40</sub> in the detergent-insoluble fraction when compared with vehicle-treated mice (Figure 2B). Conversely, no significant changes in detergent-soluble Aβ<sub>40</sub> and detergent-soluble and detergent-insoluble Aβ<sub>42</sub> were detected (Figure 2, A, C, and D). Confirming these data, the IHC analysis demonstrated increased Aβ<sub>40</sub> immunoreactivity in the subiculum, hippocampus, dentate gyrus, cortex, and thalamus of R715-treated mice, whereas Aβ<sub>42</sub> levels were unaffected by B<sub>1</sub>R blockade (Figure 2, E–G). Moreover, R715 administration resulted in strikingly increased thioflavin S-positive fibrillar Aβ deposition (Figure 2, H and I), thus demonstrating an important role for the B<sub>1</sub>R in Aβ accumulation.

We next aimed to determine the underlying mechanism by which B<sub>1</sub>R regulates Aβ deposition in Tg-SwDI brain. As shown in Figure 3, A and B, blockage of B<sub>1</sub>R did not change levels of APP or the balance between APP proteolytic C-terminal fragments (CTF)β (C99) and CTFα (C83). In addition, expression levels of β-secretase enzyme BACE1 and α-APP cleaving enzymes ADAM10 and ADAM17 were

unaltered by R715. Finally, the B<sub>1</sub>R antagonist was not capable of affecting the major putative Aβ clearance pathways, with no changes in LRP1 and APOE expression observed, and in one of the major Aβ-degrading enzymes, neprilysin (Figure 3, C and D). These data suggest that the B<sub>1</sub>R modulates Aβ accumulation through a mechanism independent of the regulation of Aβ production or BBB- and protease-mediated clearance.

### Bradykinin B<sub>1</sub>R Blockade Reduces Neuroinflammation in Tg-SwDI

The extensive fibrillar Aβ deposition present in cerebral blood vessels of Tg-SwDI is associated with a strong neuroinflammatory reaction.<sup>19,20,32</sup> Corroborating these data, we observed pronounced levels of GFAP-positive astrocytes and CD11b-, CD68-, CD45-, and Iba-1-positive microglia in vehicle-treated mice (Figure 4, A–D), particularly in areas with abundant 6E10-positive Aβ deposits, as demonstrated by colocalization studies (Figure 4, C and D). More important, R715 administration resulted in strikingly reduced GFAP, CD11b, CD68, CD45, and Iba-1 immunoreactivities compared with vehicle-treated mice (Figure 4, A–D). These data show that B<sub>1</sub>R plays an essential role in the glial cell activation observed in Tg-SwDI mice.

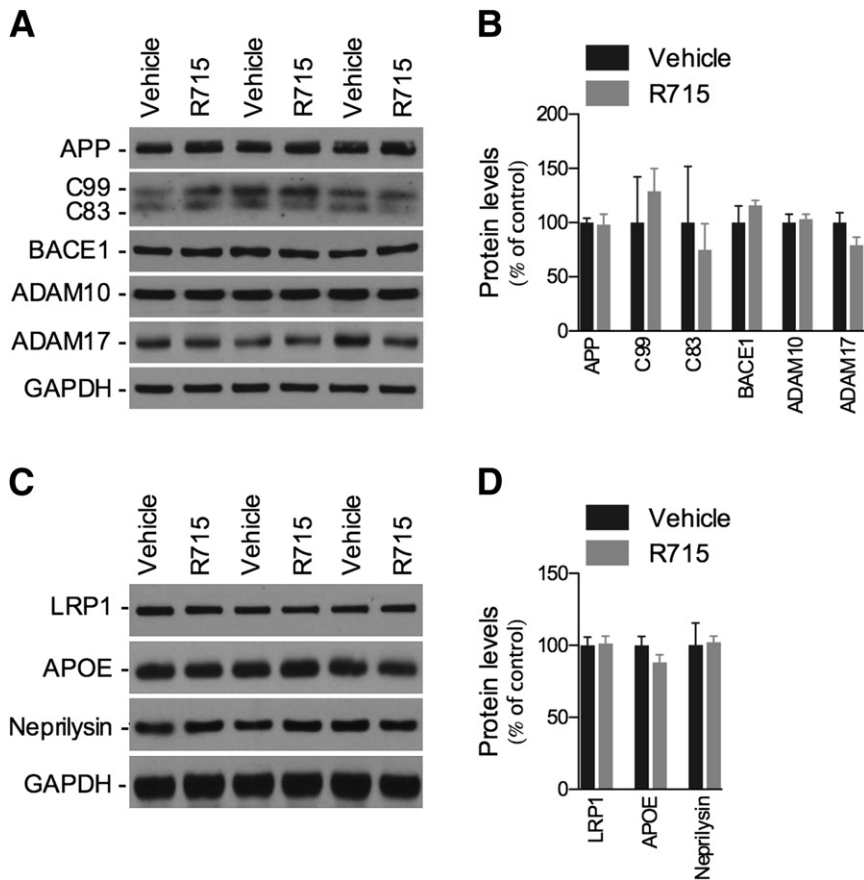


**Figure 3** B<sub>1</sub>R blockade is not associated with changes in APP processing or in levels of LRP1, APOE, and neprilysin in Tg-SwDI mice. Representative blots (A) and quantitative results (B) of Western blot analysis showing that R715 administration (1 mg/kg, s.c., 8 weeks) causes no changes in the levels of APP, APP C-terminal fragments C99 and C83, or APP-cleaving enzymes BACE1, ADAM10, and ADAM17, compared with vehicle-treated animals. C and D: Effect of R715 treatment on the expression of LRP1, APOE, and neprilysin. GAPDH levels were used as loading controls. The values represent means  $\pm$  SEM ( $N = 6$  to 8).

The inflammatory molecules observed in Tg-SwDI brains may be actively expressed by reactive microglia and astrocytes, found in intimate association with cerebral microvascular amyloid.<sup>20,33</sup> Because B<sub>1</sub>R antagonism reduced glial cell activation, we sought to determine whether the administration of R715 could also affect the levels of inflammatory mediators. Our data demonstrate that R715 administration reduces the activation of the pro-inflammatory transcription factor NF- $\kappa$ B, without affecting the anti-inflammatory receptors, liver X receptor and peroxisome proliferator-activated receptor  $\gamma$ , as shown by the marked decrease in phosphorylated-p65 NF- $\kappa$ B levels compared with vehicle-treated mice (Figure 5, A and B). On the other hand, the expression of matrix metalloproteinase-9 was not affected by the treatment (Figure 5, A and B). In addition, the production of 40 different cytokines/chemokines was profiled using a cytokine array, and drastically reduced levels of IL-1 $\alpha$ , IL-1 $\beta$ , tumor necrosis factor- $\alpha$ , CXCL1, CXCL10, chemokine ligand (CCL) 2, CCL3, C5a, and tissue inhibitor of metalloproteinases-1 were found in R715-treated versus vehicle-treated mice (Figure 5C).

#### Bradykinin B<sub>1</sub>R Blockade Is Not Associated with Cognitive Alterations in Tg-SwDI

Finally, we attempted to determine whether the effects of B<sub>1</sub>R blockade on A $\beta$  deposition and neuroinflammation were

associated with changes in cognitive function by using the novel object and novel place recognition tasks, which are believed to be primarily dependent on cortex and hippocampus, respectively.<sup>34,35</sup> Notably, no significant difference was found between control and R715-treated mice (1 mg/kg, s.c., 8 weeks) in the exploration of the nonfamiliar object in the novel object recognition task. Likewise, R715 treatment resulted in no significant change in novel place recognition task performance (data not shown).

#### Discussion

In the present study, we demonstrated that A $\beta$  deposition in Tg-SwDI mouse brain is associated with a significant up-regulation of the B<sub>1</sub>R. The pharmacological antagonism of the receptor markedly increases the deposition of A $\beta$  in the brain, and this event is accompanied by decreased activation of glial cells and a reduction in the levels of pro-inflammatory molecules, suggesting an important role for B<sub>1</sub>R in the regulation of A $\beta$  responses and neuroinflammation in AD.

The Tg-SwDI mouse is a unique model in that it develops extensive fibrillar A $\beta$  deposits primarily in cerebral microvessels, whereas A $\beta$  deposits in the brain parenchyma are predominantly diffuse. In addition, abundant reactive astrocytes and activated microglia are strongly associated with the microvascular fibrillar A $\beta$  deposits, together with

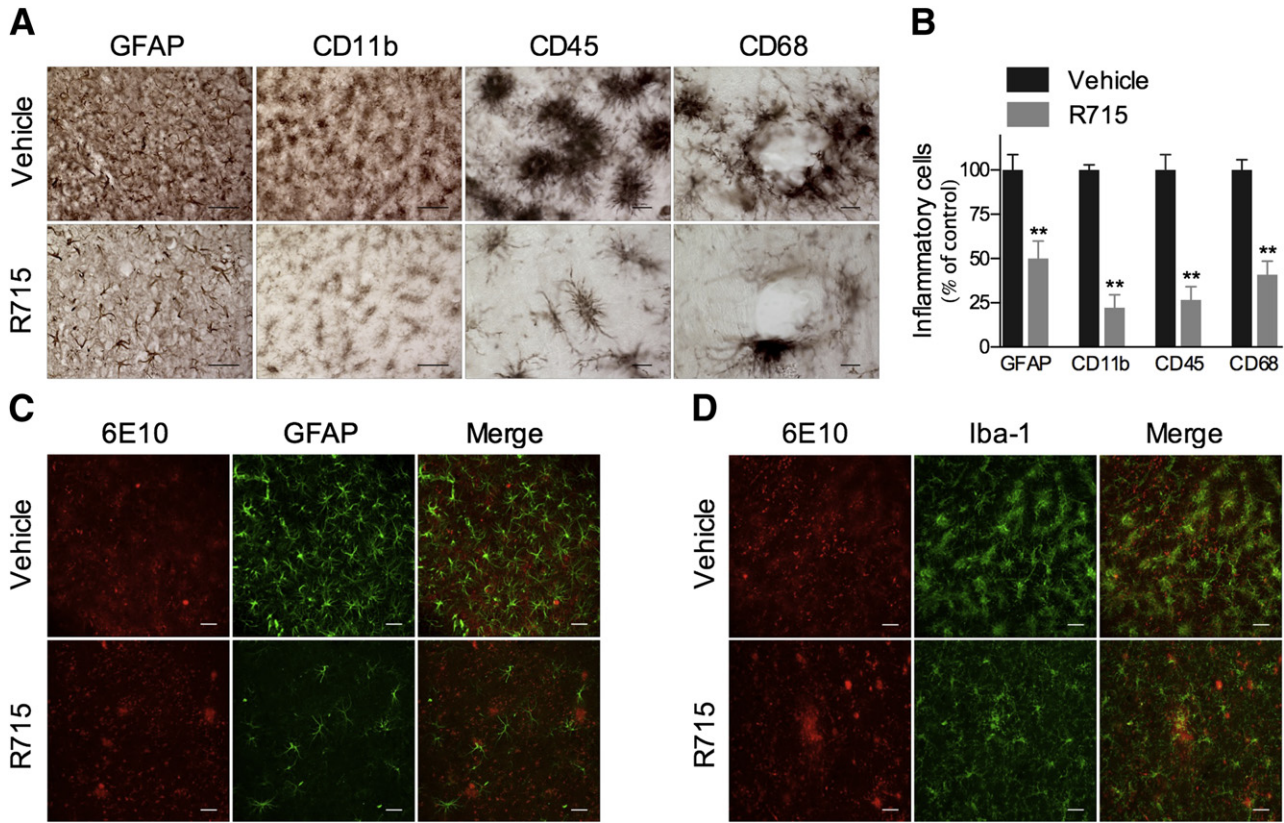


**Figure 4** B<sub>1</sub>R blockade reduces glial cell activation in Tg-SwDI mice. **A** and **B**: Tg-SwDI mouse brains s.c. treated with 1 mg/kg R715 for 8 weeks exhibited a significant decrease in GFAP-positive astrocytes and CD68-, CD11b-, and CD45-positive microglia immunoreactivity versus vehicle-treated animals. Confocal analysis showing the colocalization of 6E10-positive Aβ deposits (red) and GFAP-positive astrocytes (green) (**C**) or Iba-1-positive microglia (green) (**D**). Representative photomicrographs were taken from the subiculum. Scale bars: 50 μm (GFAP and CD11b); 10 μm (CD45 and CD68); and 25 μm (**C** and **D**). The values represent means ± SEM (N = 5 to 6). \*\*P < 0.01. The graph represents the average of inflammatory cells on the cortex, dentate gyrus, subiculum, and thalamus.

increased levels of pro-inflammatory mediators.<sup>20,32,36</sup> The pro-inflammatory cytokines tumor necrosis factor-α and IL-1β can induce the up-regulation of the B<sub>1</sub>R both *in vitro* and *in vivo*.<sup>37–40</sup> In addition, we and others have previously demonstrated that Aβ<sub>40</sub> induces the up-regulation of the B<sub>1</sub>R in rodents, particularly in brain regions related to

cognitive behavior, suggesting that this receptor could be up-regulated in AD brain.<sup>27–29</sup> In support of this hypothesis, we found significantly increased levels of the B<sub>1</sub>R in the brain of Tg-SwDI mice compared with nTg animals, with neurons, astrocytes, and vascular cells showing up-regulated expression of the receptor, predominantly in

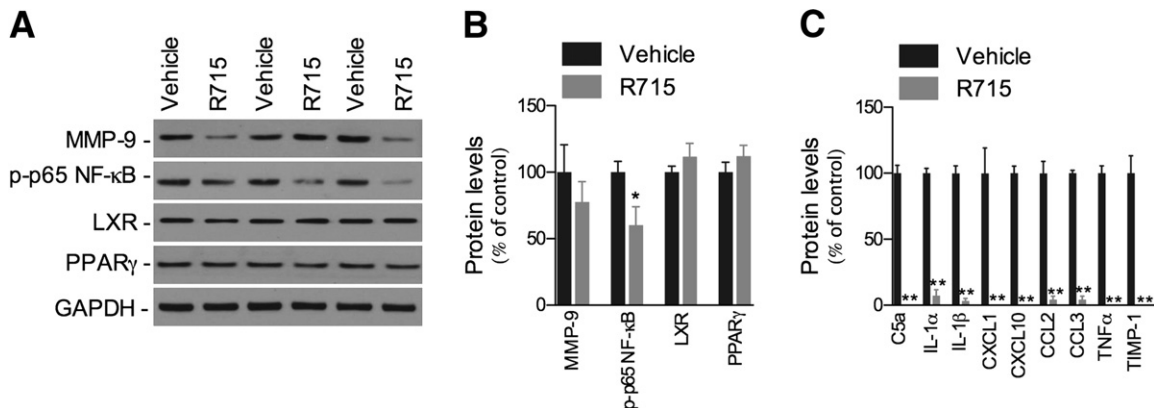


**Figure 5** B<sub>1</sub>R blockade reduces neuroinflammation in Tg-SwDI mice. Representative blots (**A**) and quantitative results (**B**) of Western blot analysis demonstrating that s.c. administration of 1 mg/kg R715 for 8 weeks reduces the levels of phosphorylated-p65 NF-κB, but not of liver X receptor, peroxisome proliferator-activated receptor γ, or matrix metalloproteinase (MMP)-9, compared with vehicle-treated mice. GAPDH levels were used as loading controls. **C**: Cytokine expression determined by a cytokine array. Data were quantified as pixel density and presented as percentage of vehicle-treated controls. The values represent means ± SEM (N = 4 to 8). \*P < 0.05, \*\*P < 0.01.

areas of A $\beta$  deposition. A similar pattern of expression has been reported in multiple sclerosis, focal cerebral ischemia, and traumatic brain injury. Of great relevance, blockade of the B<sub>1</sub>R has been shown to be beneficial in these inflammatory disease models, although conflicting data have been reported for multiple sclerosis.<sup>31,41–46</sup>

In our study, pharmacological blockade of the B<sub>1</sub>R resulted in a marked elevation in the amount of insoluble A $\beta$ <sub>40</sub>, particularly in the cortex, subiculum, dentate gyrus, and thalamus, together with increased thioflavin S–positive fibrillar A $\beta$  deposits. To our knowledge, this is the first report showing that the B<sub>1</sub>R is an important regulator of A $\beta$  deposition in the brain. Interestingly, this effect appears to be independent of alterations in A $\beta$  production, because no change in the levels of APP, ADAM10, ADAM17, BACE1, C99, and C83 were found in R715-treated mice. More important, C99 is produced by the cleavage of APP by  $\beta$ -secretase and is a marker of amyloidogenic APP processing, whereas cleavage of APP by  $\alpha$ -secretase generates the C83 fragment, a marker of the nonamyloidogenic APP processing.<sup>2</sup> In addition, we found no changes in the expression of LRP1, APOE, and neprilysin, suggesting that B<sub>1</sub>R activation is not involved in the control of BBB- and protease-mediated A $\beta$  clearance pathways. However, the presence of the dual Dutch and Iowa mutations within A $\beta$  in Tg-SwDI mice results in low efficiency for LRP1-mediated transport across the BBB, and may possibly contribute to resistance to degradation by insulin-degrading enzyme and neprilysin.<sup>16,47,48</sup> Therefore, additional experiments using other APP transgenic models are necessary to better characterize the effect of B<sub>1</sub>R on A $\beta$  clearance. In addition, changes in uncharacterized clearance mechanisms cannot be excluded.

To gain further insight into the underlying mechanisms through which B<sub>1</sub>R regulates A $\beta$  accumulation, the effect of B<sub>1</sub>R blockade on glial cell activation was examined. Notably, the activation of both microglia and astrocytes was markedly suppressed by R715, providing evidence for the critical role of the B<sub>1</sub>R in the control of glial cell responses in Tg-SwDI mice. Several studies suggest that microglia and astrocytes have a role in internalizing and degrading A $\beta$ .<sup>49–51</sup> Recently, it was demonstrated that increased infiltration and activation of neuroinflammatory cells, such as microglia/macrophages, might contribute to the clearance of pre-existing A $\beta$  deposits after an ischemic lesion in Tg-SwDI mice.<sup>52</sup> Similar results were found in other transgenic mouse models. In J20 APP-Tg mice, the inhibition of microglial activation using minocycline resulted in significantly increased A $\beta$  deposition in the hippocampus. Similarly, toll-like receptor 4–dependent microglial activation was shown to be necessary to restrict A $\beta$  deposition and preserve cognitive function in TgAPP<sup>swe</sup>/PS1<sup>dE9</sup> mice.<sup>53,54</sup> Thus, one possible scenario is that the accumulation of activated glial cells induced by B<sub>1</sub>R up-regulation contributes to a reduction in A $\beta$  deposition in the brain through a phagocytic-mediated clearance mechanism.

Despite their role in clearing A $\beta$  deposits, glial cells can also secrete several pro-inflammatory mediators, including cytokines, chemokines, complement proteins, and free radicals, in response to A $\beta$  stimulation, therefore contributing to the inflammatory component of AD.<sup>55,56</sup> Herein, we demonstrated that the activation of the B<sub>1</sub>R is required for the activation of NF- $\kappa$ B, a transcription factor important for pro-inflammatory mediator production in response to A $\beta$ .<sup>57</sup> Consistent with this finding, we observed a striking inhibition of the expression of a series of pro-inflammatory proteins, including the cytokines IL-1 $\alpha$ , IL-1 $\beta$ , and tumor necrosis factor- $\alpha$ , and the complement protein C5a. The administration of R715 has been shown to reduce the production of cytokines in response to focal brain injury.<sup>45</sup> Our data also demonstrate that B<sub>1</sub>R is implicated in the production of chemokines, because we found reduced levels of CXCL1, CXCL10, CCL2, and CCL3 in R715-treated brains. More important, we and others have shown that the production of CCL3 is involved in glial accumulation in response to A $\beta$ .<sup>54,58</sup> In addition, a recent study demonstrated that activation of CCR2 by CCL2 is essential for microglia-mediated A $\beta$  clearance in Tg2576 mice, because CCR2 deficiency markedly impairs accumulation of microglia to sites of A $\beta$  deposition and accelerates early disease progression.<sup>59</sup>

Interestingly, despite the effect of B<sub>1</sub>R blockade on glial responses and neuroinflammation, we could not find any improvement in the cognitive performance of Tg-SwDI mice on both novel object and novel place recognition tasks. Recently, it was demonstrated that minocycline, an anti-inflammatory treatment targeted for microglial activation, can improve cognitive deficits in this same animal model, although the authors found no changes in the accumulation and distribution of A $\beta$ .<sup>33</sup> In our previous studies using an A $\beta$ <sub>40</sub>-injected mouse model of neuroinflammation, the up-regulation of the B<sub>1</sub>R was shown to play an important role in the cognitive deficits induced by the peptide, as demonstrated by enhanced Morris water maze performance after B<sub>1</sub>R blockade.<sup>27</sup> However, there are significant differences between the mouse models used in our previous and current studies that may account for the differences observed. Previously, we used a model of intracerebral A $\beta$ <sub>40</sub> injection in which A $\beta$  is rapidly cleared and does not accumulate in the brain, whereas the Tg-SwDI model used in the current study presents robust cerebral microvascular accumulation of fibrillar A $\beta$ . In view of that, it is possible to suggest that the lack of cognitive alterations found in our study is related to the increased accumulation of A $\beta$ <sub>40</sub> in response to R715 treatment, because both early-onset accumulation of microvascular amyloid and neuroinflammation are associated with behavioral deficits in Tg-SwDI mice.<sup>19</sup>

Taken together, our data reveal an important role for the B<sub>1</sub>R in neuroinflammation and in the control of A $\beta$  accumulation in Tg-SwDI mice, possibly through the regulation of glial cell responses. Therefore, the modulation of the receptor may represent a novel therapeutic approach for AD.



## Acknowledgment

We thank Dr. William E. Van Nostrand (Stony Brook University, Stony Brook, NY) for providing the Tg-SwDI mice.

## References

- Selkoe DJ: Alzheimer's disease: genes, proteins, and therapy. *Physiol Rev* 2001, 81:741–766
- Querfurth HW, LaFerla FM: Alzheimer's disease [Erratum appears in *N Engl J Med* 2011, 364:588]. *N Engl J Med* 2011, 362:329–344
- Tanzi RE, Bertram L: Twenty years of the Alzheimer's disease amyloid hypothesis: a genetic perspective. *Cell* 2005, 120:545–555
- Weller RO, Subash M, Preston SD, Mazanti I, Carare RO: Perivascular drainage of amyloid-beta peptides from the brain and its failure in cerebral amyloid angiopathy and Alzheimer's disease. *Brain Pathol* 2008, 18:253–266
- Kumar-Singh S: Cerebral amyloid angiopathy: pathogenetic mechanisms and link to dense amyloid plaques. *Genes Brain Behav* 2008, 7(Suppl 1):67–82
- Neuropathology Group, Medical Research Council Cognitive Function and Aging Study: Pathological correlates of late-onset dementia in a multicentre, community-based population in England and Wales: Neuropathology Group of the Medical Research Council Cognitive Function and Ageing Study (MRC CFAS). *Lancet* 2001, 357:169–175
- Thal DR, Ghebremedhin E, Orantes M, Wiestler OD: Vascular pathology in Alzheimer disease: correlation of cerebral amyloid angiopathy and arteriosclerosis/lipohyalinosis with cognitive decline. *J Neuropathol Exp Neurol* 2003, 62:1287–1301
- Attems J, Jellinger KA: Only cerebral capillary amyloid angiopathy correlates with Alzheimer pathology: a pilot study. *Acta Neuropathol* 2004, 107:83–90
- Eikelenboom P, Veerhuis R, Familian A, Hoozemans JJ, van Gool WA, Rozemuller AJ: Neuroinflammation in plaque and vascular beta-amyloid disorders: clinical and therapeutic implications. *Neurodegener Dis* 2008, 5:190–193
- Bailey TL, Rivara CB, Rocher AB, Hof PR: The nature and effects of cortical microvascular pathology in aging and Alzheimer's disease. *Neurol Res* 2004, 26:573–578
- Thal DR, Grinberg LT, Attems J: Vascular dementia: different forms of vessel disorders contribute to the development of dementia in the elderly brain. *Exp Gerontol* 2012, 47:816–824
- Van Broeckhoven C, Haan J, Bakker E, Hardy JA, Van Hul W, Wehnert A, Vegter-Van der Vlis M, Roos RA: Amyloid beta protein precursor gene and hereditary cerebral hemorrhage with amyloidosis (Dutch). *Science* 1990, 248:1120–1122
- Levy E, Carman MD, Fernandez-Madrid IJ, Power MD, Lieberburg I, van Duinen SG, Bots GT, Luyendijk W, Frangione B: Mutation of the Alzheimer's disease amyloid gene in hereditary cerebral hemorrhage, Dutch type. *Science* 1990, 248:1124–1126
- Grabowski TJ, Cho HS, Vonsattel JP, Rebeck GW, Greenberg SM: Novel amyloid precursor protein mutation in an Iowa family with dementia and severe cerebral amyloid angiopathy. *Ann Neurol* 2001, 49:697–705
- Davis J, Xu F, Deane R, Romanov G, Previti ML, Zeigler K, Zlokovic BV, Van Nostrand WE: Early-onset and robust cerebral microvascular accumulation of amyloid beta-protein in transgenic mice expressing low levels of a vasculotropic Dutch/Iowa mutant form of amyloid beta-protein precursor. *J Biol Chem* 2004, 279:20296–20306
- Deane R, Wu Z, Sagare A, Davis J, Du Yan S, Hamm K, Xu F, Parisi M, LaRue B, Hu HW, Spijkers P, Guo H, Song X, Lenting PJ, Van Nostrand WE, Zlokovic BV: LRP/amyloid beta-peptide interaction mediates differential brain efflux of A $\beta$  isoforms. *Neuron* 2004, 43:333–344
- Davis J, Xu F, Miao J, Previti ML, Romanov G, Ziegler K, Van Nostrand WE: Deficient cerebral clearance of vasculotropic mutant Dutch/Iowa double A $\beta$  in human A $\beta$ PP transgenic mice. *Neurobiol Aging* 2006, 27:946–954
- Vasilevko V, Xu F, Previti ML, Van Nostrand WE, Cribbs DH: Experimental investigation of antibody-mediated clearance mechanisms of amyloid-beta in CNS of Tg-SwDI transgenic mice. *J Neurosci* 2007, 27:13376–13383
- Xu F, Grande AM, Robinson JK, Previti ML, Vasek M, Davis J, Van Nostrand WE: Early-onset subicular microvascular amyloid and neuroinflammation correlate with behavioral deficits in vasculotropic mutant amyloid beta-protein precursor transgenic mice. *Neuroscience* 2007, 146:98–107
- Miao J, Xu F, Davis J, Otte-Holler I, Verbeek MM, Van Nostrand WE: Cerebral microvascular amyloid beta protein deposition induces vascular degeneration and neuroinflammation in transgenic mice expressing human vasculotropic mutant amyloid beta precursor protein. *Am J Pathol* 2005, 167:505–515
- Moreau ME, Garbacki N, Molinaro G, Brown NJ, Marceau F, Adam A: The kallikrein-kinin system: current and future pharmacological targets. *J Pharmacol Sci* 2005, 99:6–38
- Calixto JB, Medeiros R, Fernandes ES, Ferreira J, Cabrini DA, Campos MM: Kinin B1 receptors: key G-protein-coupled receptors and their role in inflammatory and painful processes. *Br J Pharmacol* 2004, 143:803–818
- Leeb-Lundberg LM, Marceau F, Müller-Esterl W, Pettibone DJ, Zuraw BL: International union of pharmacology, XLV: classification of the kinin receptor family: from molecular mechanisms to pathophysiological consequences. *Pharmacol Rev* 2005, 57:27–77
- Regoli D, Barabe J: Pharmacology of bradykinin and related kinins. *Pharmacol Rev* 1980, 32:1–46
- Marceau F, Regoli D: Bradykinin receptor ligands: therapeutic perspectives. *Nat Rev Drug Discov* 2004, 3:845–852
- Campos MM, Leal PC, Yunes RA, Calixto JB: Non-peptide antagonists for kinin B1 receptors: new insights into their therapeutic potential for the management of inflammation and pain. *Trends Pharmacol Sci* 2006, 27:646–651
- Prediger RD, Medeiros R, Pandolfo P, Duarte FS, Passos GF, Pesquero JB, Campos MM, Calixto JB, Takahashi RN: Genetic deletion or antagonism of kinin B(1) and B(2) receptors improves cognitive deficits in a mouse model of Alzheimer's disease. *Neuroscience* 2008, 151:631–643
- Viel TA, Lima Caetano A, Nasello AG, Lancelotti CL, Nunes VA, Araujo MS, Buck HS: Increases of kinin B1 and B2 receptors binding sites after brain infusion of amyloid-beta 1-40 peptide in rats. *Neurobiol Aging* 2008, 29:1805–1814
- Amaral FA, Lemos MT, Dong KE, Bittencourt MF, Caetano AL, Pesquero JB, Viel TA, Buck HS: Participation of kinin receptors on memory impairment after chronic infusion of human amyloid-beta 1-40 peptide in mice. *Neuropeptides* 2010, 44:93–97
- Tsuchida S, Miyazaki Y, Matsusaka T, Hunley TE, Inagami T, Fogo A, Ichikawa I: Potent antihypertrophic effect of the bradykinin B2 receptor system on the renal vasculature. *Kidney Int* 1999, 56:509–516
- Schulze-Toppoff U, Prat A, Prozorovski T, Siffrin V, Paterka M, Herz J, Bendix I, Ifergan I, Schadock I, Mori MA, Van Horsen J, Schroter F, Smorodchenko A, Han MH, Bader M, Steinman L, Aktas O, Zipp F: Activation of kinin receptor B1 limits encephalitogenic T lymphocyte recruitment to the central nervous system. *Nat Med* 2009, 15:788–793
- Miao J, Vitek MP, Xu F, Previti ML, Davis J, Van Nostrand WE: Reducing cerebral microvascular amyloid-beta protein deposition diminishes regional neuroinflammation in vasculotropic mutant amyloid precursor protein transgenic mice. *J Neurosci* 2005, 25:6271–6277
- Fan R, Xu F, Previti ML, Davis J, Grande AM, Robinson JK, Van Nostrand WE: Minocycline reduces microglial activation and improves behavioral deficits in a transgenic model of cerebral microvascular amyloid. *J Neurosci* 2007, 27:3057–3063

34. Barker GR, Bird F, Alexander V, Warburton EC: Recognition memory for objects, place, and temporal order: a disconnection analysis of the role of the medial prefrontal cortex and perirhinal cortex. *J Neurosci* 2007, 27:2948–2957
35. Dere E, Huston JP, De Souza Silva MA: The pharmacology, neuroanatomy and neurogenetics of one-trial object recognition in rodents. *Neurosci Biobehav Rev* 2007, 31:673–704
36. Fan R, DeFilippis K, Van Nostrand WE: Induction of complement proteins in a mouse model for cerebral microvascular A beta deposition. *J Neuroinflammation* 2007, 4:22
37. Campos MM, de Souza GE, Ricci ND, Pesquero JL, Teixeira MM, Calixto JB: The role of migrating leukocytes in IL-1 beta-induced up-regulation of kinin B(1) receptors in rats. *Br J Pharmacol* 2002, 135:1107–1114
38. Zhang Y, Adner M, Cardell LO: IL-1beta-induced transcriptional up-regulation of bradykinin B1 and B2 receptors in murine airways. *Am J Respir Cell Mol Biol* 2007, 36:697–705
39. Murakami M, Ohta T, Ito S: Interleukin-1beta enhances the action of bradykinin in rat myenteric neurons through up-regulation of glial B1 receptor expression. *Neuroscience* 2008, 151:222–231
40. Campos MM, Souza GE, Calixto JB: Modulation of kinin B<sub>1</sub> but not B<sub>2</sub> receptors-mediated rat paw edema by IL-1 $\beta$  and TNF $\alpha$ . *Peptides* 1998, 19:1269–1276
41. Su J, Cui M, Tang Y, Zhou H, Liu L, Dong Q: Blockade of bradykinin B2 receptor more effectively reduces postischemic blood-brain barrier disruption and cytokines release than B1 receptor inhibition. *Biochem Biophys Res Commun* 2009, 388:205–211
42. Göbel K, Pankratz S, Schneider-Hohendorf T, Bittner S, Schuhmann MK, Langer HF, Stoll G, Wiendl H, Kleinschnitz C, Meuth SG: Blockade of the kinin receptor B1 protects from autoimmune CNS disease by reducing leukocyte trafficking. *J Autoimmun* 2011, 36:106–114
43. Prat A, Biernacki K, Pouly S, Nalbantoglu J, Couture R, Antel JP: Kinin B1 receptor expression and function on human brain endothelial cells. *J Neuropathol Exp Neurol* 2000, 59:896–906
44. Trabold R, Erös C, Zweckberger K, Relton J, Beck H, Nussberger J, Müller-Esterl W, Bader M, Whalley E, Plesnila N: The role of bradykinin B(1) and B(2) receptors for secondary brain damage after traumatic brain injury in mice. *J Cereb Blood Flow Metab* 2010, 30:130–139
45. Raslan F, Schwarz T, Meuth SG, Austinat M, Bader M, Renné T, Roosen K, Stoll G, Sirén AL, Kleinschnitz C: Inhibition of bradykinin receptor B1 protects mice from focal brain injury by reducing blood-brain barrier leakage and inflammation. *J Cereb Blood Flow Metab* 2010, 30:1477–1486
46. Austinat M, Braeuninger S, Pesquero JB, Brede M, Bader M, Stoll G, Renne T, Kleinschnitz C: Blockade of bradykinin receptor B1 but not bradykinin receptor B2 provides protection from cerebral infarction and brain edema. *Stroke* 2009, 40:285–293
47. Morelli L, Llovera R, Gonzalez SA, Affranchino JL, Prelli F, Frangione B, Ghiso J, Castano EM: Differential degradation of amyloid beta genetic variants associated with hereditary dementia or stroke by insulin-degrading enzyme. *J Biol Chem* 2003, 278:23221–23226
48. Van Vickle GD, Esh CL, Dausgs ID, Kokjohn TA, Kalback WM, Patton RL, Luehrs DC, Walker DG, Lue LF, Beach TG, Davis J, Van Nostrand WE, Castano EM, Roher AE: Tg-SwDI transgenic mice exhibit novel alterations in AbetaPP processing, Abeta degradation, and resilient amyloid angiopathy. *Am J Pathol* 2008, 173:483–493
49. Matsunaga W, Shirokawa T, Isobe K: Specific uptake of Abeta1-40 in rat brain occurs in astrocyte, but not in microglia. *Neurosci Lett* 2003, 342:129–131
50. Simard AR, Soulet D, Gowing G, Julien JP, Rivest S: Bone marrow-derived microglia play a critical role in restricting senile plaque formation in Alzheimer's disease. *Neuron* 2006, 49:489–502
51. Pihlaja R, Koistinaho J, Kauppinen R, Sandholm J, Tanila H, Koistinaho M: Multiple cellular and molecular mechanisms are involved in human A $\beta$  clearance by transplanted adult astrocytes. *Glia* 2011, 59:1643–1657
52. Van Nostrand WE, Davis J, Previti ML, Xu F: Clearance of amyloid- $\beta$  protein deposits in transgenic mice following focal cerebral ischemia. *Neurodegener Dis* 2012, 10:108–111
53. Seabrook TJ, Jiang L, Maier M, Lemere CA: Minocycline affects microglia activation, Abeta deposition, and behavior in APP-tg mice. *Glia* 2006, 53:776–782
54. Song M, Jin J, Lim JE, Kou J, Pattanayak A, Rehman JA, Kim HD, Tahara K, Lalonde R, Fukuchi K: TLR4 mutation reduces microglial activation, increases A $\beta$  deposits and exacerbates cognitive deficits in a mouse model of Alzheimer's disease. *J Neuroinflammation* 2011, 8:92
55. Li C, Zhao R, Gao K, Wei Z, Yin MY, Lau LT, Chui D, Hoi Yu AC: Astrocytes: implications for neuroinflammatory pathogenesis of Alzheimer's disease. *Curr Alzheimer Res* 2011, 8:67–80
56. McGeer EG, McGeer PL: Neuroinflammation in Alzheimer's disease and mild cognitive impairment: a field in its infancy. *J Alzheimers Dis* 2010, 19:355–361
57. Combs CK, Karlo JC, Kao SC, Landreth GE:  $\beta$ -Amyloid stimulation of microglia and monocytes results in TNF $\alpha$ -dependent expression of inducible nitric oxide synthase and neuronal apoptosis. *J Neurosci* 2001, 21:1179–1188
58. Passos GF, Figueiredo CP, Prediger RD, Pandolfo P, Duarte FS, Medeiros R, Calixto JB: Role of the macrophage inflammatory protein-1alpha/CC chemokine receptor 5 signaling pathway in the neuro-inflammatory response and cognitive deficits induced by beta-amyloid peptide. *Am J Pathol* 2009, 175:1586–1597
59. El Khoury J, Toft M, Hickman SE, Means TK, Terada K, Geula C, Luster AD: Ccr2 deficiency impairs microglial accumulation and accelerates progression of Alzheimer-like disease. *Nat Med* 2007, 13:432–438